SUB-SECTION I e

SHEARING STRENGTH AND EQUILIBRIUM OF SOILS

I e 12 SHEARING STRENGTH AND WATER CONTENT, A COMPLEMENT TO THE SHEARING THEORY

R. HAEFELI

Institute for Hydraulic Research and Soil Mechanics,
of the Swiss Federal Institute of Technology, Zurich.

I. DEFINITION OF THE PROBLEM.

The possibilities of influencing the internal friction and the shearing strength of fine-grained kinds of soil by altering the water content are as varied as the nature of water itself. This variety is on the one hand conditioned by the fact that the water contained in the soil may occur in three different forms, namely free, molecularly combined, or chemically combined. On the other hand, in connection with that we have the fact that the water, according to circumstances, may act at one time as lubricant and at another time as an antilubricant. This becomes particularly clear when the shearing stress is investigated with the material not only in the saturated state, but also unsaturated.

Known experimental and theoretical works 1) 2) 3) 4) have been concerned hitherto almost exclusively with clearing up the shearing strength conditions in saturated loose sediments. But, for rounding off the shearing theory, the behaviour of moist materials should be examined over the whole range between the dry and the saturated states. The particulars given in section II of the present study serve this purpose, but make no claim to be complete.

In practice it is often necessary to determine the shearing strength and internal friction of moist, non-saturated loose sediments, as for instance when endeavouring to control earth slides, whose frequency is generally greatest in the late autumn, when heavy rain-falls occur after lengthy periods of drought. The water entering into the shrinkage cracks causes an increasing moistening through the material until saturation is reached, and effects a corresponding change in the shearing strength and the internal friction of the soil 5). The behaviour of unsaturated loose sediments also plays a decisive part in ceramics, in the brickmaking industry and above all in foundry technique. The moulding sands used in a foundry are worked-up with water contents which lie far below the saturation point, so that here all three phases (solid material, water and air) must be considered in their reciprocal action on each other.

After considering the transition shown between the moist and saturated states, a short survey is given in section III regarding the latest state of the shearing theory developed for saturated loose sediments; this will be more closely investigated in another place 6). As an extension of that, a simple regular relation was found regarding the change in water content of fine-grained loose sediments during shearing operations.

II. SHEARING STRENGTH OF UNSATURATED LOOSE SEDIMENTS AS A FUNCTION OF THE WATER CONTENT.

1. Theoretical considerations.

In order to investigate the dependence of the shearing strength on the water content below the saturated limit, we start with the dry powdery state of the loose sediment. To this powder more and more water is added step by step, the kneaded material is compressed at a given pressure, for instance $\sigma = 1$ kg/cm^2, and after consolidation sheared slowly under the same normal stress. The shear strengths thereby obtained are plotted as a function of the water content and may give the curves designated with A-B in Fig. 1. At a certain water content w_I measured after the shearing, the saturation point B is finally reached. A still higher water content could only be obtained in the closed system by the formation of stressed pore water. In the open system on the other hand, the sample will always drain again during the shearing operation to the final water content w_I corresponding to the point B.

Further the question arises as to what happens if the water is withdrawn from a compressed and fully consolidated sample with water content w_I, in order to make the process gone through reversible. It will then be found that the process here is not reversible, since saturation at first remains maintained by evaporation when water is carefully withdrawn 7). The sample shrinks, passing through the first phase of the shrinking process, during which time the capillary pressure gradually decreases until its upper limit, designated shrinking pressure by Terzaghi, is reached. The shearing strength corresponding to this phase is given by the part of the curve B - E, which is identical with the saturation limit. If the removal of water is continued after the shrinking pressure (E) has been reached, whereby the second phase of the shrinking process starts, the sample will no longer be saturated, since its pores fill partly with air. The increase in the capillary tensions becomes gradually less and the shearing strength passes through the curve E -F, whose position and shape depend on the properties of the loose sediment in question. Thus the hysteresis loop arises which is illustrated purely diagrammatically in Fig. 1. Its shape is not more closely known, and will depend not only on the material, but also on the conditions under which the test is conducted. Further, if the consolidation pressure would be chosen higher, for instance $\sigma = 2$ kg/cm^2 instead of $\sigma = 1$, the whole hysteresis loop would lie correspondingly higher. All hysteresis loops have a common saturation limit, the formulating of which will be investigated in the following pages.

According to the shear theory for saturated loose sediments treated in section III, the following relation holds good between the shearing strength s and the maximum principal stress σ_I arising during the shearing (cf. Fig. 5) 8):

$$s = \sigma_I \cdot \operatorname{tg} \varphi_0 = \frac{\operatorname{tg} \varphi_0}{1 + \operatorname{tg} \varphi_0 \cdot \operatorname{tg}\left(\frac{\pi}{4} + \frac{\varphi_r}{2}\right)} \cdot \sigma_I = \alpha \cdot \sigma_I \qquad (1)$$

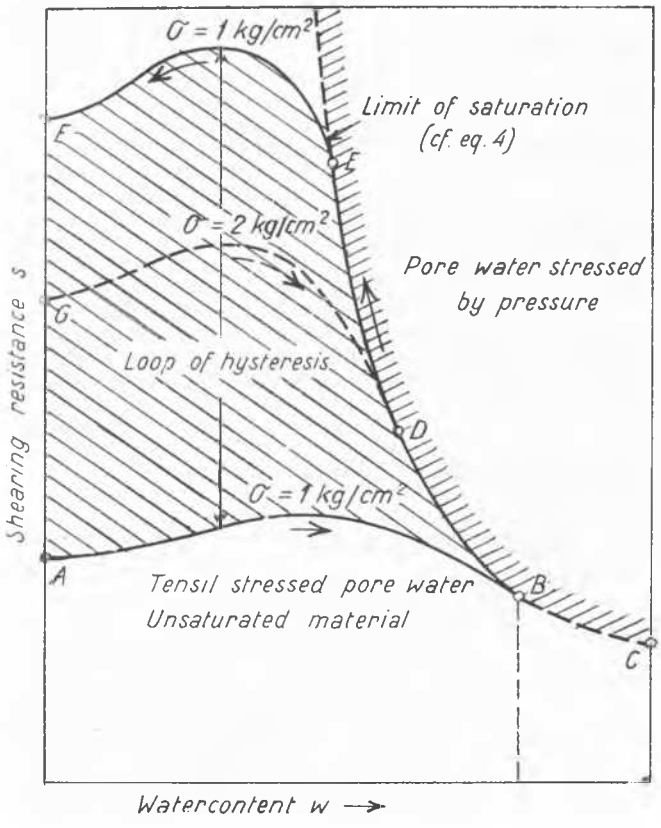

Relation between shearing resistance and water content (diagram).

FIG.1

For a given material and a given type of structure as parameter, the following relation may on the other hand be derived between the equivalent consolidating pressure σ_I, which occurs here as the major principal stressing during the shearing, and the corresponding water content w_I present at the end of the slow shearing process:

$$w_I = w_1 - \Delta_e \cdot \ln \lambda_I \left(w_1 + \frac{\gamma_w}{\gamma_s} \right) \quad ; \quad \lambda_I = \frac{\sigma_I}{\sigma_1} \qquad (2)$$

$$\sigma_I = \sigma_1 \cdot e^{\beta} \qquad \beta = \frac{w_1 - w_I}{\Delta_e \left(w_1 + \frac{\gamma_w}{\gamma_s} \right)} \qquad (3)$$

where:
w_I = water content of the material for the equivalent consolidating pressure σ_1 = 1 kg/cm².
Δ_e = Coefficient of compressibility 14).
γ_s = Specific gravity of the solid substance.
γ_w = Specific gravity of the water.

By substituting from equation (3) in equation (1), the desired equation of the saturating limit is obtained in the form;

$$s = \alpha \cdot e^{\beta} \cdot \sigma_1 \qquad \sigma_1 = 1 \text{ kg/cm}^2 \qquad (4)$$

2. Tests.

For investigating the relation between shearing strength and water content in the region of the lower branch of the above-mentioned hysteresis loop, three different materials were prepared with the necessary quantity of water, pressed several times through a sieve of 5 mm mesh, and then allowed to stand for at least 24 hours in a saturated atmosphere. The samples thus prepared were consolidated and then slowly sheared in a ring shearing apparatus. We are indebted to Dr. A. von Moos for his collaboration in carrying out and evaluating the tests 9).

a) Test materials.

The most important properties of the three investigated materials are summarised in table 1

TABLE 1

Properties of the test materials.

Material	Kaolin	Alumina	Quartz
Grain distribution in percentage by weight %	K	T	Q
Fractions:			
0,2 - 0,02 mm	1,0	98,0	13
0,02 - 0,002 mm	40,0	1,5	51,5
< 0,002 mm	59,0	0,5	35,5
Chemical analysis			
Silicic acid SI O_2 %	46,25	-	98,82
Alumina Al_2O_3 %	39,28	100	0,06
Iron, lime, magnesium, alkalis and water %	14,47	-	1,12
Consistency limits			
flow limit f in %	61,0		
plastic limit a in %	33,3	incoherent	incoherent
Coefficient of plasticity P = f - a	27,7		
Coefficient of compressibility Δ_e %	6,6	0,73	1,37
Coefficient of permeability k_{10} in cm/sec	$2,2.10^{-8}$	$3,2.10^{-4}$	$2,2.10^{-6}$
Capillary rise in cm	100	1,1	12

b) Test results.

The test results are illustrated in Fig. 2, 3 and 4. Corresponding to the differences in the properties of the materials which can be seen from table 1, the three materials behaved very differently during the shearing test.

With the kaolinite-clay an addition of water at first caused a slight diminishing of the shearing strength determined for a given normal stress; with higher water contents on the other hand, there was an increase. The maximum shearing strength was reached in a region with a water content of 19 - 26%. With still higher water contents the internal friction diminishes greatly up to saturation value (cf. table 2 and Fig. 2, 3a).

In the shearing strength of moist kaolinite-clay, the capillary forces undoubtedly play a predominant part. They explain the occurence of a maximum shearing strength with a definite water content. The great drop in the shearing strength when approaching the saturated state, which occurs in spite of an intense compacting (cf. Fig. 2 and 4), may be attributed mainly to the gradual elimination of the capillary forces. The low shearing strength in the saturated state, in comparison with dry alumina powder, is on the other hand to be explained by the lubricating action of the absorbed liquid films,which make themselves very marked with the large specific surfaces of the kaolinite-clay and to a great extent prevent direct contact of the grains.

TABLE 2

Internal friction of Kaolinite.clay ; $tg\ \varphi = s/\sigma$

Normal stress σ in kg/cm^2		0,5	1	2	3
Dry	$tg\ \varphi$	0,81	0,72	0,72	0,65
Moist	$tg\ \varphi_{max.}$	0,90	0,85	0,76	0,73
Saturated	$tg\ \varphi_s$	0,34	0,31	0,29	0,28
$tg\ \varphi_{max}$ in % of $tg\ \varphi_s$		270	270	260	260

The maximum value of the shearing strength and/or the internal friction is consequently approximately 2.6 - 2.7 times greater than the saturation value, which at the same time represents the minimum value. The slight reduction of the internal friction with increasing pressure, which could be determined at all the water contents investigated, was more pronounced in the dry and moist states than when saturation was reached.

The alumina, which may be described as practically without cohesion as compared with the highly coherent kaolinite-clay, showed a polar contrary behaviour. As can be seen from Fig. 3b), the shearing strength here was smallest in the dry state, but on the other hand greatest in the saturated state, although the difference did not exceed 20%.

The quartz takes up a middle position with respect to its behaviour under shearing tests, as was already to be expected from the figures in table 1. For comparison see table 3.

TABLE 3

Internal friction of quartz: $tg\ \varphi = s/\sigma$

Normal stress σ in kg/cm^2		0,5	1	2
Dry	$tg\ \varphi$	0,65	0,71	0,74
Moist	$tg\ \varphi_{max}$	0,86	0,81	0,90
Saturated	$tg\ \varphi_s$	0,64	0,80	0,84
$tg\ \varphi_{max}$ in % of $tg\ \varphi_s$		135	101	107

In order to explain physically the partly contradictory behaviour of the three materials in the region of incomplete saturation, it should first of all be remembered that two quite different influences collaborate in shearing strength, namely on the one hand the friction caused by the external forces, and on the other hand the cohesion. The latter again in its turn consists of two components: the friction caused by the capillary forces and the actual structural resistance, which is conditioned by the separate particles interlocking and by the shearing strength of the absorbed liquid films 10).

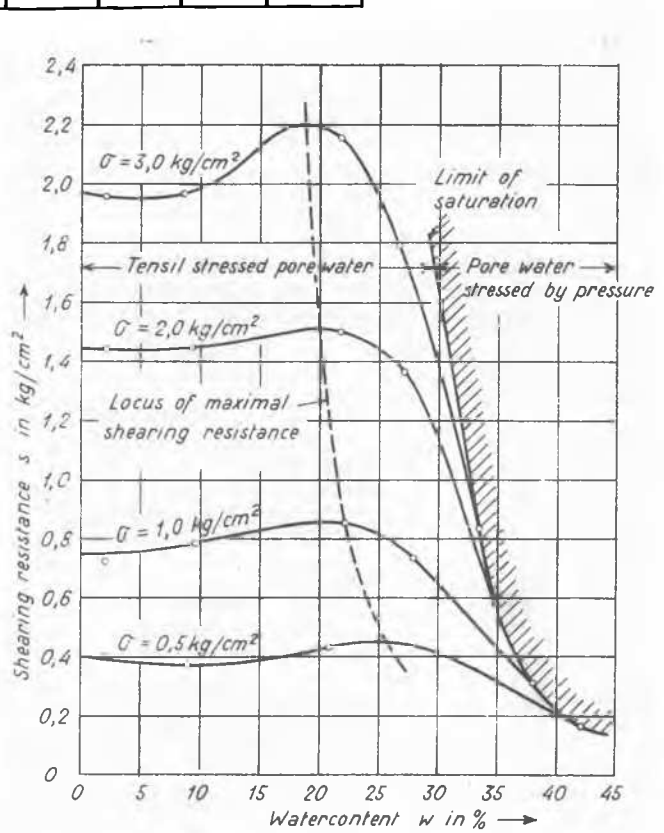

Shearing resistance as a function of the water content for Kaolinite-clay.

FIG. 2

The behaviour of the quartz, to some extent similar but much less marked, becomes understandable when the lesser fineness of its grains and the correspondingly smaller capillary rise are taken into consideration. That quartz in the saturated state has a somewhat higher average shearing strength than in the dry state, appears to be explained by the predominant influence of the structural resistance. which increases with the consolidation.

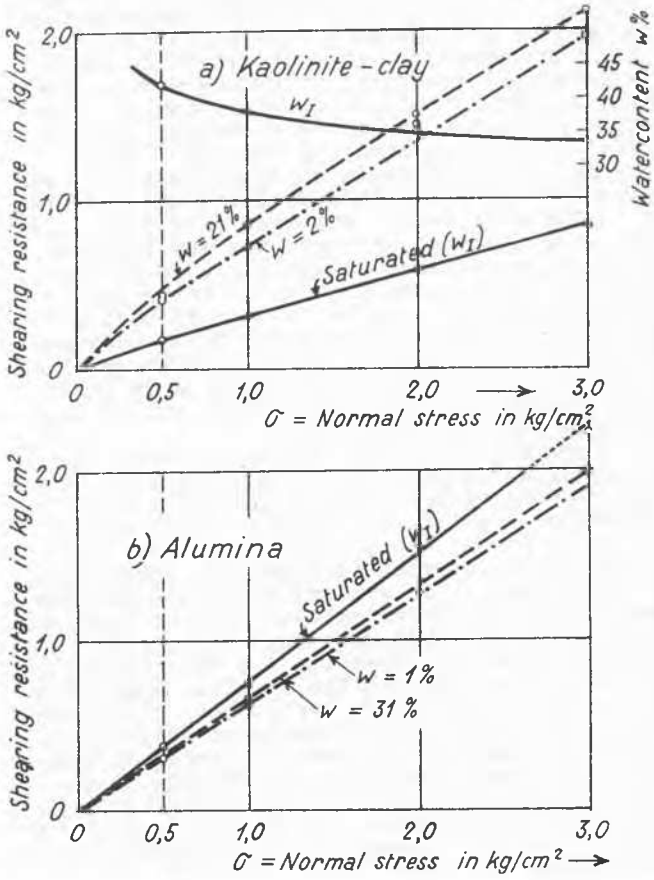

Shearing tests for different water contents (kaolinite-clay and alumina).

FIG.3

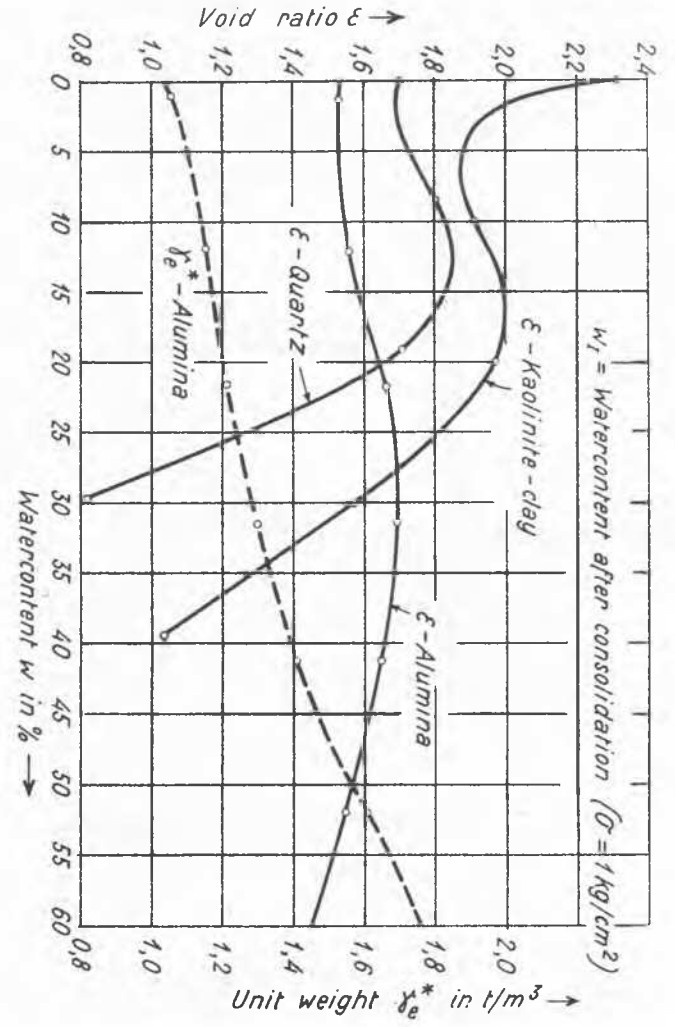

Void ratio ε as a function of the water content for $\sigma = 1$ kg/cm² and unsaturated material.

FIG.4

With the alumina, whose void ratio according to Fig. 4 changes only slightly with increasing water content, the maximum shearing strength in the saturated state is explained by the poor lubricating action of the very thin liquid films, which are not capable of preventing the grains from coming into direct contact with each other. The water in this case acts rather as an antilubricating medium in consequence of its permitting additional adhesion. Also with the very small capillary rise in this material the capillary forces are so slight that their elimination when the saturated limit is reached is of no importance, (cf. table 1).

Finally it is to be noted that the saturated limit calculated according to equation 4 agrees very well with the curve determined by experiment.

III. SHEARING STRENGTH AND INTERNAL FRICTION IN THE SATURATED STATE.

1. Shearing strength as a function of the normal stressing.

In the saturated state the connection between the shearing strength and the normal stressing acting on the shearing surface is given essentially by the following two elements:

φ_s = angle of apparent internal friction

φ_r = angle of true internal friction.

To understand the shearing diagram illustrated in Fig. 5, it is necessary to distinguish between shearing operations in open and in closed systems. In an open system, in which the water can issue freely during the shearing so that no stressed pore water can be present, the shearing strength is more or less directly proportional to the normal stress σ. It will be represented by the a-line, which is inclined to the horizontal at an angle φ_s. As is known, the shearing strength is composed of two different elements, the friction r and the cohesion c, both of which increase proportionally to the normal stress σ:

$$s = c + r = \sigma (\operatorname{tg} \varphi_c + \operatorname{tg} \varphi_r) = \sigma \cdot \operatorname{tg} \varphi_s \qquad (5)$$

The cohesion c, and also the water content w_I, measured at the end of the slow shearing process, are conditioned by the consolidation of the material which takes place during slow shearing under the influence of the major principal stress σ_1, the decisive factor for consolidation.

In contrast to the open system, in the closed system it is assumed that no alteration in water content and therefore also no change in the volume of the material take place during the shearing process. Under this assumption the cohesion c, as measure of the respective compacting condition, also remains

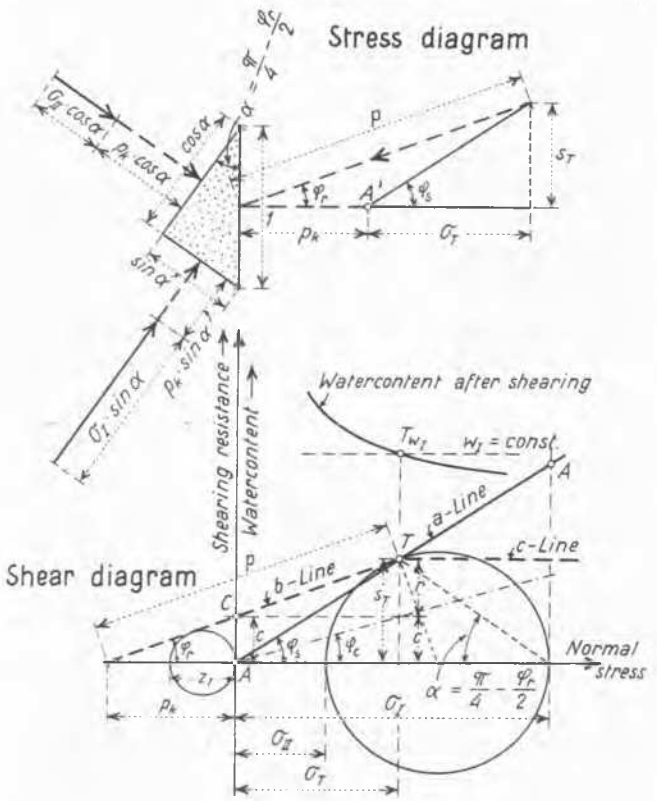

Shearing diagram for saturated material.

FIG.5

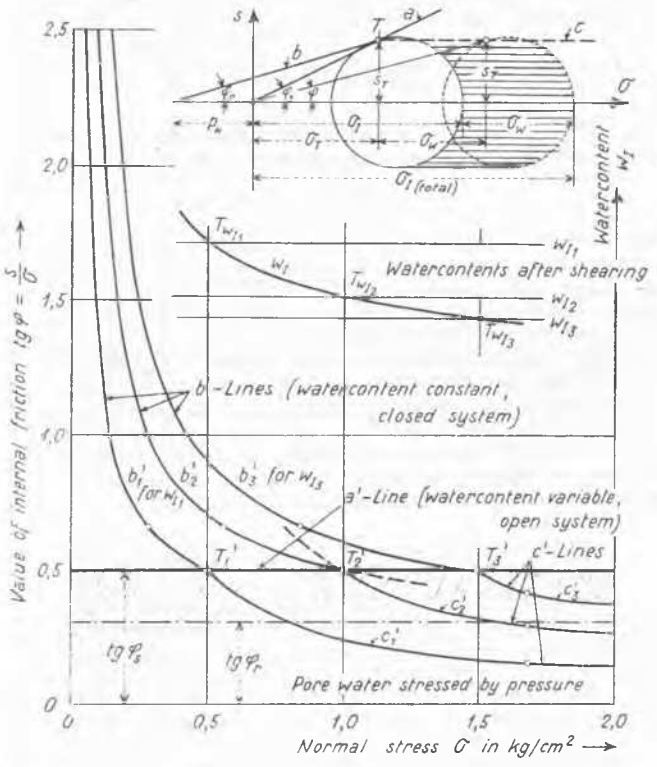

Internal friction for saturated material.

FIG.6

constant. As long as there is no pore water stressed by pressure, the shearing strength follows the Coulomb straight line for constant cohesion (b-line). Water content and cohesion are in this case given by the equivalent consolidation pressure. In order that the maximum principal stressing occurring during the shearing may not become greater than σ_1, the normal stressing (shearing pressure) may not exceed a definite limiting value σ_T. If it does so, its difference in comparison with the equivalent consolidation pressure will be taken by the pore water (stressed pore water). If $\sigma > \sigma_T$, the shearing strength thereby remains practically unchanged, namely $s = s_T$ (c-line). From this it follows that an infinite number of approximately parallel b-c-lines belong to one single a-line, and the points of intersection T of all the b-c-lines lie on the a-line. To each point T there corresponds a definite water content w_I, measured at the end of the shearing process, (Fig. 5).

From Fig. 5 it can further be seen that the shearing diagram is to be understood as a true picture of the stressfigure on the unit surface of a prismatic element of the material, in so far as the p_K values are inserted as additional hydrostatic pressure stressings. The experimental determination of the diagram can be effected advantageously by the combined adoption of two different apparatus, namely the ring shearing apparatus for shearing tests in the open system and the triaxial apparatus for tests in the closed system 8). The theoretical and experimental bases of this shearing theory, which have been developed in parallel with the investigations of Krey-Tiedemann 3) and Hvorslev 1), and described in different publications 4), 8) 11), are to be found collected together in a publication in the English language to which we here refer 6).

2. Internal friction as a function of the normal stressing.

If, instead of the shearing strength s, the internal friction $\operatorname{tg}\varphi = \frac{s}{\sigma}$ is plotted as a function of the normal stressing σ, the picture illustrated in Fig. 6 is obtained. Corresponding to the a-line of Fig. 5, which is decisive for the open system, we have here the horizontal a'-line, with $\operatorname{tg}\varphi = \operatorname{tg}\varphi_s = \text{constant}$. For the closed system on the other hand, the internal friction can be represented by a group of curves, with the water content w_I as parameter. Instead of the b-lines of Fig. 5, we have the b'-lines of Fig. 6. These are equilateral hyperbolae, whose equation is:

$$\operatorname{tg}\varphi = \frac{c}{\sigma} + \operatorname{tg}\varphi_r \quad ; \quad (\operatorname{tg}\varphi - \operatorname{tg}\varphi_r)\cdot\sigma = c = \text{const.} \quad (6)$$

The horizontal line $\operatorname{tg}\varphi = \operatorname{tg}\varphi_r$ appears as the common horizontal asymptote. For stressed pore water on the other hand, the c'-lines hold good; they form a second group of hyperbolae with the two coordinate axes as asymptotes and have the equation:

$$\operatorname{tg}\varphi = \frac{s_\tau}{\sigma} \quad ; \operatorname{tg}\varphi \cdot \sigma = s_\tau = \sigma_\tau \cdot \operatorname{tg}\varphi_s = \text{const.} \quad (7)$$

3. Reduction of the water content during shearing.

For the open system there is theoretically a simple connection between the consolidation of the material during slow shearing and the corresponding change in water content (Fig. 7). By the shearing operation we thereby understand the whole change in tension between static pressure and the state at rupture

Before the shearing operation, the normal stress σ is identical with the first principal stress, which gradually increases during the shearing process to the value σ_1, rotating simultaneously about the angle

$$\left(\frac{\pi}{4}+\frac{\varphi_r}{2}\right)$$

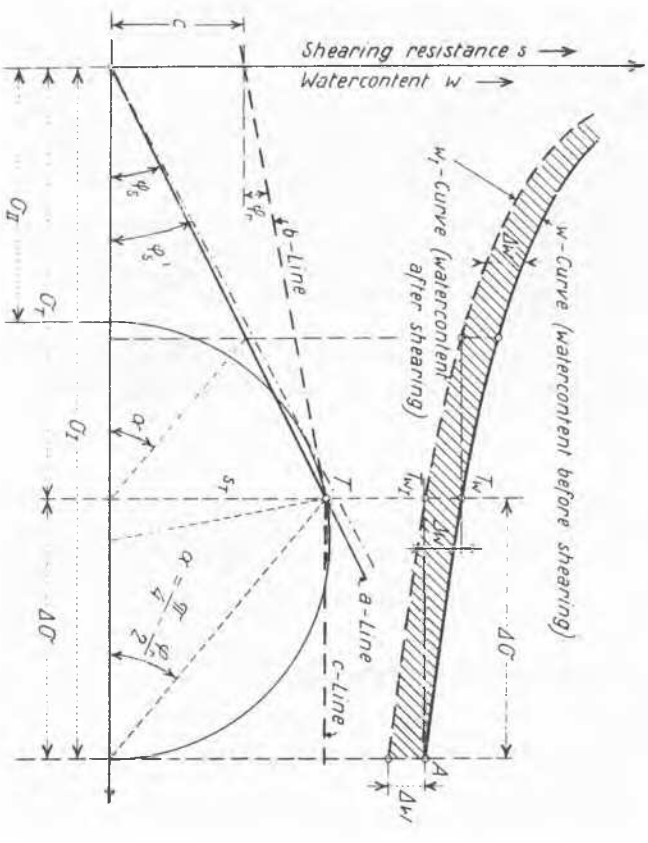

Change in water content during the shearing of saturated loose sediments (fine-grained soil).

FIG.7

From Fig. 7 it can be seen that this increase, indicated with $\Delta\sigma = \sigma_1 - \sigma$, is proportional to the normal stress, since it holds good that:

$$\frac{\Delta\sigma}{\sigma} = \operatorname{tg}\varphi_s \cdot \operatorname{tg}\left(\frac{\pi}{4}+\frac{\varphi_r}{2}\right) = u \qquad (8)$$

On the other hand the specific settlement, calculated as previously, is as follows: 4) 14)

$$\Delta_i = \Delta_e \cdot \ln\lambda_i \quad ; \quad \lambda_i = \frac{\sigma_i}{\sigma} \; ; \; \frac{d(\Delta_i)}{d\lambda_i} = \frac{\Delta_e}{\lambda_i} \; ; \; \frac{d(\Delta_i)}{d\sigma} = \frac{\Delta_e}{\sigma} \qquad (9)$$

$$d(\Delta_i) = \frac{d\sigma}{\sigma}\cdot\Delta_e \qquad (10)$$

If a finite increase in settlement is considered instead of an infinitely small change in the specific settlement, the following holds good approximately:

$$\Delta(\Delta_i) \cong \frac{\Delta\sigma}{\sigma}\cdot\Delta_e = u\cdot\Delta_e \qquad (\text{cf. eq. } 8) \qquad (11)$$

This equation states that the consolidation (a-line), effected in a given material by slow shearing in the open system, is a constant magnitude independent of the normal stressing σ. Thereby it has only been assumed that during the shearing process - apart from the shearing surfaces - no disturbance in structure occurs, as is generally the case for clays with a decided tendency to form surfaces of slip. Our considerations therefore may not be transferred to any sandy materials in which the shearing process causes possibly an increase in porosity or on the contrary a break-down of structure, so that phenomena occur which led A. Casagrande to introduce the conception of the critical void ratio 13).

On the other hand, since the volume of water issuing from the material, in consequence of the consolidation by shearing, is identical with the change in volume of the material itself, or stands in a definite relation to it, it follows further that also the change in water content Δ_w is a constant magnitude independent of the normal stressing. It may be calculated approximately as follows:

$$\Delta_w \cong -\Delta_e\left(w_1+\frac{\gamma_w}{\gamma_s}\right)u = -\Delta_e\frac{\gamma_w}{\gamma_s}(1+\varepsilon_1)u = \text{const.} \qquad (12)$$

where:

w_1, ε_1 = water content and void ratio for the equivalent consolidation pressure $\sigma = 1$ kg/cm^2.

γ_w, γ_s = specific gravities of the water and the solid substance respectively.

In Fig. 7 the regularity of the change in water content during the shearing test, which still requires checking by experiment, finds its expression in the curve of water content w_1 (after shearing) being displaced downwards in comparison with the curve w (before shearing), by the fixed value Δ_w, so that the two curves run in parallel.

IV. CONCLUSIONS.

1) In the unsaturated state of the loose sediments the dependence of the shearing strength on the water content is to a large extent conditioned by the grain distribution and mineralogical composition. With fine-grained, clayey materials and with a given normal stress, the shearing strength reaches its maximum value at a definite water content, after which it falls off greatly until the saturation point is reached (Fig. 1 and 2). Also the direction of the altering of the water content (addition or removal of water) plays here a decisive part (hysteresis loop). Further, while the shearing strength of cohesive materials in the unsaturated state is as a rule greater than in the saturated state, the contrary may be the case with non-cohesive types of soil (cf. alumina, Fig. 3).

2) In the saturated state the general shearing diagram is given by the angles of the apparent and the real internal friction (φ_s and φ_r). In the closed system the dependence of the shearing strength on the normal stressing is represented by the single straight line (a-line) inclined at φ_s, in the open system by a group of broken straight lines (b-c-lines), each of which represents a definite water content and/or a definite equivalent consolidation pressure as parameter. With plastic loose sediments (loam and clay) the shearing operation, causes a consolidation, characteristic for the material in question and independent of the normal tension, and thereby also a constant change in water content which can be calculated approximately (eq. 12). This theory is based on the fact, that the possible consolidation of a fine grained saturated soil only depends of the major principal stress.

BIBLIOGRAPHY.

1) M.J. Hvorslev: Ueber die Festigkeitseigenschaften gestörter bindiger Böden. Kopenhagen 1937.

2) K. v. Terzaghi: The shearing resistance of saturated soils and the angle between the planes of shear. Proceedings of the international conference on soil mechanics. Vol. I, p. 54, Cambridge Mass. 1936.
3) B. Tiedemann: Ueber die Schubfestigkeit bindiger Böden. Die Bautechnik. Vol. 15,Nr. 30 & 33, 1937.
4) R. Haefeli: Mechanische Eigenschaften von Lockergesteinen. Schweiz. Bauzeitung Bd. III Nr. 24 & 26, 1938.
5) L. Bendel und R. Rückli: Die Erdrutsche von Emmenegg und Dallenwil. Strasse und Verkehr 1937, Nr. 15 & 16.
6) Ch. Schaerer - W. Schaad - R. R. Haefeli: Contribution to the shearing theory. Second International Conference on Soil Mechanics. Rotterdam 1948.
7) R. Haefeli - G. Amberg: Contribution to the theory of shrinking. Second International Conference on Soil Mechanics. Rotterdam 1948.
8) R. Haefeli und Ch. Schaerer: Der Triaxialapparat. Schweiz. Bauzeitung Bd. 128, Nr. 5, 6, 7 1946. Mitteilung Nr. 11 der Versuchsanstalt für Wasserbau und Erdbau ETH Zürich.
9) R. Haefeli und A. von Moos: Scherfestigkeit von Lockergesteinen in Funktion des Wassergehaltes im Bereich unvollständiger Sättigung. Interner, unveröffentlichter Bericht der Versuchsanstalt für Wasserbau und Erdbau ETH Zürich 1941.
10) W. Bernatzik: Baugrund und Physik, Zürich 1947.
11) R. Haefeli: Erdbaumechanische Probleme im Lichte der Schneeforschung. Schweiz. Bauzeitung Bd. 123, 1944 (Mitteilung Nr. 7 der Versuchsanstalt für Wasserbau an der ETH Zürich).
12) J.-P. Daxelhofer: Remarques sur la résistance au cisaillement des sols et son importance dans quelques cas particuliers. Bulletin technique de la Suisse romande, 1944, No. 25.
13) A. Casagrande and N. Carillo: Shear failure of anisotropic materials. Publications from the graduate school of engineering. Soil Mechanics, Series No. 22. Harvard University 1944.
14) R. Haefeli: On the compressibility of preconsolidated soil layers. Second International Conference on Soil Mechanics, Rotterdam 1948.

-o-o-o-o-o-o-

I e 13

ON THE BEARING POWER OF SOIL IN A TWO-DIMENSIONAL PROBLEM

T. MIZUNO
Prof. of Engineering College, Kyushu University, Fukuoka, Japan

SUMMARY

In this paper, the author reports of a theoretical study on the ultimate bearing power of grounds and the shapes of sliding surfaces in a two-dimensional case, taking into consideration the body force due to the soil weight.

1. GENERAL ASSUMPTIONS.

In Fig. 1 let p be the load intensity from a structure having the width 2b and q be the surcharge intensity outside the structure. When the base of the structure is located at the depth t from the ground surface, the soil weight γt is taken as q; where γ is the unit weight of the soil.

We will begin with sand grounds.

From the experimental results, we assume that, at the instant of sliding, the wedge part ABC is pushed down together with the load along the sliding planes AC and BC of Rankine's active earth pressure, and the region NBD reaches to the state of passive earth pressure. Then, if ρ is the angle of internal friction, we get

$$\angle ABC = \theta_0 = \frac{\pi}{4} + \frac{\rho}{2} \tag{1}$$

and

$$\angle NBD = \pi - \theta_0 = \frac{\pi}{4} - \frac{\rho}{2} \tag{2}$$

Along any radial line through B, the passive earth pressure due to q distributes uniformly and that due to γ distributes proportionally to the distance from B. Therefore, at the instant of sliding, the load p must be resisted by the following two forces; the one, that is independent to the radial distance r from B, and the other, that is proportional to r.

Now, we divide p into two parts p' and p" which are resisted by the above forces respectively.

$$p = p' + p'' \tag{3}$$

At the sliding, the resisting forces along the sliding planes AC and BC should make an angle ρ with the normals to these planes and can be assumed to consist of the following three parts as shown in Fig. 1.

The first of them is the active earth pressure due to the body force of sand and its components are as follows.

$$\left.\begin{aligned} \sigma_{\theta_0}^{(a)} &= \gamma(1-k)\, r \sin^2\theta_0 + \Lambda_0 \\ \tau_{r\theta_0}^{(a)} &= -\gamma(1-k)\, r \sin^2\theta_0 \cos\theta_0 \\ \sigma_{r_0}^{(a)} &= \gamma(1-k)\, r \sin\theta_0 \cos^2\theta_0 + \Lambda_0 \end{aligned}\right\} \tag{4}$$

where,

$$k = \frac{1-\sin\rho}{1+\sin\rho} \tag{5}$$

and

$$\Lambda_0 = -\gamma r \sin\theta_0 \tag{6}$$